THE JOURNAL OF BIOLOGICAL CHEMISTRY VOL. 285, NO. 5, pp. 3289–3299, January 29, 2010

Prevention of CCAAT/Enhancer-binding Protein β DNA Binding by Hypoxia during Adipogenesis*[S]

Received for publication, August 25, 2009, and in revised form, October 27, 2009 Published, JBC Papers in Press, November 25, 2009, DOI 10.1074/jbc.M109.059212

Young-Kwon Park[1] **and Hyunsung Park**[2]

From the Department of Life Science, University of Seoul, Siripdae-gil 13, Dongdaemun-gu, Seoul 130-743, Republic of Korea

Upon exposure to adipogenesis-inducing hormones, confluent 3T3-L1 preadipocytes express C/EBPβ (CCAAT/enhancer binding protein β). Early induced C/EBPβ is inactive but, after a lag period, acquires its DNA-binding capability by sequential phosphorylation. During this period, preadipocytes pass the G_1/S checkpoint synchronously. Thr^{188} of C/EBPβ is phosphorylated initially to prime the factor for subsequent phosphorylation at Ser^{184} or Thr^{179} by GSK3β, which translocates into the nuclei during the G_1/S transition. Many events take place during the G_1/S transition, including reduction in $p27^{Kip1}$ protein levels, retinoblastoma (Rb) phosphorylation, GSK3β nuclear translocation, and C/EBPβ binding to target promoters. During hypoxia, hypoxia-inducible factor-1α (HIF-1α) is stabilized, thus maintaining expression of $p27^{Kip1}$, which inhibits Rb phosphorylation. Even under normoxic conditions, constitutive expression of $p27^{Kip1}$ blocks the nuclear translocation of GSK3β and DNA binding capability of C/EBPβ. Hypoxia also blocks nuclear translocation of GSK3β and DNA binding capability of C/EBPβ in HIF-1α knockdown 3T3-L1 cells that fail to induce $p27^{Kip1}$. Nonetheless, under hypoxia, these cells can block Rb phosphorylation and the G_1/S transition. Altogether, these findings suggest that hypoxia prevents the nuclear translocation of GSK3β and the DNA binding capability of C/EBPβ by blocking the G_1/S transition through HIF-1α-dependent induction of $p27^{Kip1}$ and an HIF-1α/p27-independent mechanism.

The oxygen pressure in normoxic tissue has been estimated to be 2–9% (14.4–64.8 mm Hg). As such, physiological normoxia represents a much lower oxygen concentration than that of air, which is 20% O_2. Insufficient blood circulation limits the delivery of oxygen and causes hypoxia, defined as 1–3% O_2 (1, 2). To maintain oxygen homeostasis during hypoxic stress, cells activate many signaling molecules, including hypoxia-inducible factor (HIF),[3] endoplasmic reticulum stress response, and the environment-sensing mammalian target of rapamycin (3).

HIF plays a major role in adaptive responses to hypoxia, including erythropoiesis, angiogenesis, vasodilation, and anaerobic metabolic changes by inducing such target genes encoding erythropoietin, vascular endothelial growth factor, and inducible nitric-oxide synthase as well as those of many glycolytic enzymes. HIF, which belongs to the basic helix-loop-helix-Per-Arnt-Sim (PAS) family, is a heterodimeric transcription factor consisting of two subunits, α and β. The first HIF-α isoform, HIF-1α, was identified by affinity purification, whereas HIF-2α/EPAS-1 was discovered in a homology search. Both isoforms heterodimerize with HIF-1β. In normoxia, HIF-1α becomes ubiquitinated and rapidly degraded. A ubiquitin E3 ligase, von Hippel-Lindau protein, recognizes and binds hydroxylated proline residues in HIF-1α. Proline hydroxylation of HIF-1α is catalyzed by hydroxylases specific to the factor that consume oxygen, α-ketoglutarate, vitamin C, and ferrous iron (Fe^{2+}) in the reaction (4). These cofactors are also involved in the inhibition of HIF-1α transcriptional activity by the asparaginyl hydroxylase factor-inhibiting HIF-1α (5).

Hypoxia occurs during embryogenesis, organogenesis, and in growing tumors prior to vascularization. Local hypoxic microenvironments form specific niches that modulate cell proliferation and differentiation. Recent studies have demonstrated that hypoxia regulates molecules involved in stem cell differentiation, such as Notch, β-catenin, Oct4, c-Myc, and Stra13/DEC1 (6–10). Furthermore, hypoxia has been shown to inhibit adipogenesis by repressing the transcription factor, peroxisome proliferator-activated receptor-γ2 (PPARγ2), which initiates and maintains this biological event by inducing adipocyte-specific genes. Expression of PPARγ2 as well as C/EBPα is repressed by HIF-1 through induction of the basic helix-loop-helix transcription repressor Stra13/DEC1 (10). PPARγ2 and C/EBPα are induced by adipogenic transcription factors, including C/EBPβ, C/EBPδ, and C/EBPα, which are activated sequentially by adipogenesis-inducing hormones (11). The C/EBP family is widely expressed, and its members play critical roles in regulating energy metabolism, inflammation, hematopoiesis, cellular proliferation, and differentiation. Despite this, C/EBPs are not expressed in 3T3-L1 preadipocytes in the absence of adipogenesis-inducing hormones (12–15).

2–6 h following hormonal induction, growth-arrested 3T3-L1 preadipocytes express C/EBPβ. Early induced C/EBPβ is inactive; however, 8–12 h postinduction, this factor exhibits DNA binding activity and transactivation. During this lag period, the level of cell cycle-dependent kinase inhibitor $p27^{Kip1}$ decreases, and preadipocytes progress synchronously through the G_1/S checkpoint and enter mitosis. Meanwhile, C/EBPβ undergoes sequential phosphorylation at Thr^{188} and Ser^{184} (or Thr^{179}),

* This work was supported by Korea Healthcare Technology R&D Project Grant A090616 (to H. P.).

[S] The on-line version of this article (available at http://www.jbc.org) contains supplemental Figs. 1 and 2.

[1] Supported by a Seoul Science Fellowship.

[2] To whom correspondence should be addressed. Tel.: 82-2-2210-2622; Fax: 82-2-2210-2888; E-mail: hspark@uos.ac.kr.

[3] The abbreviations used are: HIF, hypoxia-inducible factor; PAS, basic helix-loop-helix-Per-Arnt-Sim; ERK, extracellular signal-regulated kinase; PI, propidium iodide; shRNA, short hairpin RNA; FACS, fluorescence-activated cell sorting; ChIP, chromatin immunoprecipitation; PBS, phosphate-buffered saline; MCE, mitotic clonal expansion; BIO, 6-bromoindirubin-3′-oxime; MEF, mouse embryo fibroblast; Rb, retinoblastoma.

leading to conformational changes that enable dimerization and DNA binding (16). Thr^{188} is phosphorylated by p42/p44 extracellular signal-regulated kinase (ERK) and CDK2/cyclin A during the G_1 and S phases, respectively (17). Phosphorylation at this site primes C/EBPβ for subsequent phosphorylation at Ser^{184} or Thr^{179} by GSK3β, which translocates to the nucleus at the onset of S-phase.

Many reports have suggested that C/EBPβ function is coordinated with the cell cycle (18–20). During the G_1/S transition, many events take place, including reduction in $p27^{Kip1}$ levels, retinoblastoma (Rb) phosphorylation, GSK3β nuclear translocation, dual phosphorylation of C/EBPβ, and C/EBPβ binding to the PPARγ2 and C/EBPα promoters. Despite this knowledge, the cause-and-effect relationship among these events is unclear. Here, through the use HIF-1α knockdown 3T3-L1 cells, we demonstrate that hypoxia inhibits these events, which can be dissected into at least two independent processes that are distinguishable by HIF-1α.

EXPERIMENTAL PROCEDURES

Materials, Antibodies, and Plasmids—Insulin, dexamethasone, 3-isobutyl-1-methylxantine, propidium iodide (PI), Oil Red O, and puromycin were purchased from Sigma. Bovine calf serum was purchased from Invitrogen. Fetal bovine serum and Dulbecco's modified Eagle's medium and G418 were obtained from Cambrex (Charles City, IA). [α-^{32}P]dATP and [γ-^{32}P]ATP were purchased from PerkinElmer Life Sciences. Ultralink immobilized protein A/G-agarose was purchased from Pierce. Antibodies against Rb (G3-245), GSK3β, and β-catenin were acquired from BD Biosciences. Antibodies against phospho-C/EBPβ (Thr^{188}), phospho-GSK3β (Ser^{9}), phospho-Akt (Ser^{473}), Akt, phospho-ERK, ERK, and laminin A/C were obtained from Cell Signaling Technology (Beverly, MA). Anti-HIF-1α antibody was purchased from Novus Biologicals (Littleton, CO), whereas antibodies against C/EBPα (14AA), C/EBPβ (H-7), PPARγ (E-8), p27 (C-19), p21 (C-19), p300 (N-15), and α-tubulin were obtained from Santa Cruz Biotechnology, Inc. (Santa Cruz, CA).

Cell Culture and Adipogenesis of 3T3-L1 Cells—3T3-L1 (American Type Culture Collection, catalogue number CL-173) preadipocytes were maintained in Dulbecco's modified Eagle's medium containing 10% (v/v) bovine calf serum. Postconfluent 3T3-L1 cells were induced to differentiate by the addition of a standard mixture (MDI) composed of 0.5 mM 3-isobutyl-1-methylxantine, 1 μM dexamethasone, and 5 μg/ml insulin in 10% fetal bovine serum for the first 48 h. The cells were then cultured in Dulbecco's modified Eagle's medium supplemented with 10% fetal bovine serum and 5 μg/ml insulin in a humidified atmosphere of 95% air and 5% CO_2 at 37 °C. The medium was replaced every 2 days. Cells were exposed to hypoxic conditions (1% O_2) by incubation in an anaerobic incubator (model 1029, Forma Scientific, Inc.) in an atmosphere of 5% CO_2, 10% H_2, and 85% N_2 at 37 °C.

Oil Red O Staining—Confluent 3T3-L1 cells were induced to differentiate for the indicated number of days. Cells were washed once with PBS, fixed with 10% formaldehyde in PBS for 1 h at room temperature, and then washed again with PBS. Oil Red O (0.5% in isopropyl alcohol) was diluted with distilled water at a ratio of 3:2 (v/v) and incubated with the fixed cells for 30 min at 37 °C. Cells were washed with distilled water for 10 min at 37 °C. Stained lipid droplets in the cells were visualized by light microscopy.

Transfection and Retroviral Infection—To generate 3T3-L1 cells that constitutively express HIF-1α and $p27^{Kip1}$, we used a retroviral expression system (BD Biosciences). Mouse $p27^{Kip1}$ cDNA (GenBank™ accession number NM_009875) was subcloned into the retroviral vector pWZL-IRES-neo encoding Geneticin resistance, which was a generous gift from Garry Nolan (Stanford University School of Medicine, Stanford, CA). HEK293-based packaging cells (BD AmphoPack™-293 cell line) were transfected with pWZL-IRES-neo-$p27^{Kip1}$. To generate control retrovirus, the packaging cells were transfected with an empty retroviral vector. 48 h post-transfection, retrovirus was collected from the medium of packaging cells (21). 3T3-L1 cells at 50% confluence were infected with virus-containing medium in the presence of 8 μg/ml Polybrene according to the manufacturer's instructions. The infected 3T3-L1 cells were selected in the presence of 0.5 mg/ml G418. To generate HIF-1α-knockdown cells, we used a retroviral vector system (BD Biosciences). Short hairpin RNA (shRNA) against HIF-1α (5′-GATCCGTGTGAGCTCACATCTTGATTT-CAAGAGAATCAAGATGTGAGCTCACATTTTTTAGAT-CTG-3′) was inserted into the pSIREN-RetroQ vector (BD Biosciences) according to the manufacturer's instructions to generate pSIREN-RetroQ-shHIF-1α. The infected 3T3-L1 cells were selected in the presence of 5 μg/ml puromycin. To generate control retrovirus, control shRNA provided with the kit was ligated into the pSIREN-RetroQ vector.

Preparation of Nuclear Extracts—Confluent 3T3-L1 cells were induced to differentiate for the indicated times in 100-mm culture plates. Cells were washed once with cold 10 mM HEPES, pH 7.5, and then incubated in fresh buffer on ice for 15 min. Cells were harvested with MDH buffer (3 mM $MgCl_2$, 1 mM dithiothreitol, 25 mM HEPES, pH 7.5, 0.4 mM phenylmethylsulfonyl fluoride, 2 μg/ml leupeptin, and 2 μg/ml aprotinin) and Dounce homogenized (20 strokes) using a type B pestle on ice. Nuclei were isolated by centrifugation at 1,000 × *g* for 5 min at 4 °C, washed twice with MDHK buffer (3 mM $MgCl_2$, 1 mM dithiothreitol, 25 mM HEPES, pH 7.5, 100 mM KCl, 0.4 mM phenylmethylsulfonyl fluoride, 2 μg/ml leupeptin, and 2 μg/ml aprotinin) and then resuspended in HDK buffer (25 mM HEPES, pH 7.5, 1 mM dithiothreitol, 400 mM KCl, 0.4 mM phenylmethylsulfonyl fluoride, 2 μg/ml leupeptin, and 2 μg/ml aprotinin). The extracts were incubated with gentle rocking at 4 °C for 1 h and then centrifuged at 16,000 × *g* for 1 h at 4 °C. Supernatants were isolated as nuclear extracts. Protein concentrations were measured by the Bradford assay (Bio-Rad) (22).

Northern Blot Analysis and Reverse Transcription-PCR—Total RNA was isolated using an RNeasy spin column (Qiagen, Chatsworth, CA). For Northern blot analysis, total RNA (20 μg) was used. Northern blots were hybridized with α-^{32}P-labeled cDNA specific to PPARγ2, C/EBPα, or vascular endothelial growth factor as described previously (23). For reverse transcription-PCR, total RNA (1 μg) was reverse transcribed using avian myeloblastosis virus reverse transcriptase with dNTPs and random primers (Promega, Madison, WI). PCR was per-

formed using primers specific for C/EBPβ (forward, 5′-CAAGCTGAGCGACGAGTACA-3′; reverse, 5′-AAGGTTCTCAAATATACATACGCCT-3′) and for 18 S rRNA as described (24).

FACS Analysis—Confluent 3T3-L1 cells were induced to differentiate for the indicated number of hours, washed once with PBS, harvested by trypsinization, and centrifuged at 1,000 × *g* for 5 min. The cells were fixed overnight with 70% ethanol at −20 °C. The fixed cells were washed with PBS containing 2 mM EDTA and then centrifuged. The pellet was resuspended in 1 ml of PI buffer (PBS containing 50 μg/ml PI and 40 μg/ml RNase A) and incubated at room temperature for 30 min. PI-stained cells were analyzed using a BD FACSCalibur™ flow cytometer (BD Biosciences), and the data were analyzed using CellQuest (BD Biosciences).

Chromatin Immunoprecipitation (ChIP) Analysis—A ChIP assay kit was used according to the manufacturer's instructions (Millipore, Billerica, MA). 3T3-L1 preadipocytes were induced to differentiate as described. The cells were cross-linked with 1% formaldehyde at room temperature for 10 min and then washed twice with ice-cold PBS prior to harvest. Cells were resuspended in 200 μl of SDS lysis buffer (50 mM Tris-HCl, pH 8.1, containing 1% SDS, 10 mM EDTA, and protease inhibitors), incubated on ice for 10 min, and then sonicated on ice to yield DNA fragments with an average length of 0.5–1 kb. After centrifugation at 13,000 × *g* for 10 min at 4 °C, the concentration of lysate was determined by spectrophotometry. Equivalent amounts of chromatin were used for immunoprecipitation. The lysates were diluted at a ratio of 1:10 with ChIP dilution buffer (20 mM Tris-HCl, pH 8.1, containing 1% Triton X-100, 2 mM EDTA, and 150 mM NaCl) and incubated with 2 μg of salmon sperm DNA and 20 μl of protein A/G-agarose at 4 °C for 1 h. After centrifugation, 10% of the supernatant was removed as input and stored at −20 °C, and the DNA-protein complexes were immunoprecipitated with 2 μg of anti-C/EBPβ antibody (H-7) or 2 μg of anti-p300 antibody (N-15) (Santa Cruz Biotechnology, Inc.) at 4 °C overnight. The antibody-chromatin complexes were recovered by incubation with 20 μl of protein A/G-agarose. Immunocomplexes were eluted with elution buffer (1% SDS and 0.1 M $NaHCO_3$), and NaCl was added to a final concentration of 200 mM prior to overnight at 65 °C incubation to reverse cross-linking. Finally, DNA was extracted with phenol/chloroform, precipitated, and resuspended. Precipitated DNAs were amplified by PCR (30–35 cycles) and analyzed by 2% agarose gel electrophoresis. PCR products were radiolabeled by inclusion of 0.25 μCi of [α-^{32}P]dATP in the reaction mixture followed by PCR (20–25 cycles). Radiolabeled PCR products were resuspended in 8% polyacrylamide, 1× Tris borate-EDTA gels, dried, and exposed to x-ray film. The primers used for PCR were as follows: C/EBP binding site in C/EBPα promoter (GenBank™ accession number NM_007678), 5′-TCCCTAGTGTTGGCTGGAAG-3′ (forward) and 5′-CAGTAGGATGGTGCCTGCTG-3′ (reverse); C/EBP binding site in the PPARγ2 promoter (GenBank™ accession number S79407), 5′-TTCAGATGTGTGATTAGGAG-3′ (forward) and 5′-AGACTTGGTACATTACAAGG-3′ (reverse); HIF-1α binding site in the Stra13 promoter (GenBank™ accession number AF362845), 5′-aacacgtgaggctcatgt-3′ (forward) and 5′-gttaaatgggagcgagtg-3′ (reverse).

Immunofluorescence Microscopy—3T3-L1 preadipocytes (2×10^4) were plated on glass coverslips in a 24-well culture plate and cultured until confluent. The cells were then induced to differentiate as described above. Cells were washed with PBS, fixed with 4% paraformaldehyde in PBS for 20 min at room temperature, permeabilized with 0.4% Triton X-100 in PBS for 30 min, and then washed with PBST buffer (PBS containing 0.05% Tween 20). The cells were blocked in PBST buffer containing 5% bovine serum albumin for 1–2 h at room temperature. The cells were incubated overnight with anti-C/EBPβ (H-7, 1:1,000) or anti-p27 (C-19, 1:200) antibodies in PBST buffer containing 5% bovine serum albumin and washed with PBST buffer. The cells were incubated with secondary antibody conjugated to either AlexaFluor® 546 or AlexaFluor® 488 (Invitrogen) for 1 h at room temperature. Cells mounted onto coverslips were incubated with DAPI (Invitrogen) for 5 min and then washed with PBST buffer. After the coverslips were mounted on slides, stained cells were observed under a Zeiss LSM510 inverted confocal microscope according to the manufacturer's instructions.

RESULTS

Hypoxia Represses PPARγ and C/EBPα but Not C/EBPβ—To investigate the effects of hypoxia on adipogenesis, 3T3-L1 preadipocytes were induced to differentiate into mature adipocytes by hormone treatment. Staining with Oil Red O revealed lipid droplets in 3T3-L1 cells after treatment for 8 days, indicating that the preadipocytes had differentiated under normal conditions. Lipid droplets, however, were not observed in 3T3-L1 cells treated under hypoxic conditions (Fig. 1*A*). Northern and Western analyses showed that during adipogenesis, PPARγ2 and C/EBPα and their target, adiponectin, were induced under normoxic conditions but not under hypoxic conditions. In contrast, HIF-1α and its target, vascular endothelial growth factor, were induced under hypoxia (Fig. 1, *B–D*) (25). Because PPARγ2 and C/EBPα were reported to be induced by C/EBPβ, we tested whether hypoxia also abrogated this induction. Interestingly, the expression level of C/EBPβ was unaffected by hypoxic conditions (Fig. 1, *D* and *E*).

Hypoxia Inhibits the DNA Binding Ability of C/EBPβ—Next we investigated whether hypoxia affects C/EBPβ activity. Although this factor is induced early, within 4 h of the start of differentiation, it is not immediately active. C/EBPβ acquires its DNA binding ability 8–12 h postinduction (18). ChIP analyses using an anti-C/EBPβ antibody revealed that C/EBPβ binds the C/EBPα and PPARγ2 promoters *in vivo* 12 h after induction under normoxic but not hypoxic conditions (Fig. 2, *A* and *B*). To confirm this finding, we tested whether p300, a C/EBPβ coactivator, is also recruited to the promoters of C/EBPβ target genes. ChIP analyses demonstrated that p300 also occupies the endogenous promoter regions of C/EBPα and PPARγ2 at 12–24 h after hormonal induction. Like C/EBPβ, p300 does not occupy these promoter regions under hypoxic conditions. However, this coactivator was found bound to the promoter of *Stra13/DEC1*, which is induced by HIF-1/p300 in response to hypoxia (Fig. 2*C*). Interestingly, electrophoretic mobility shift

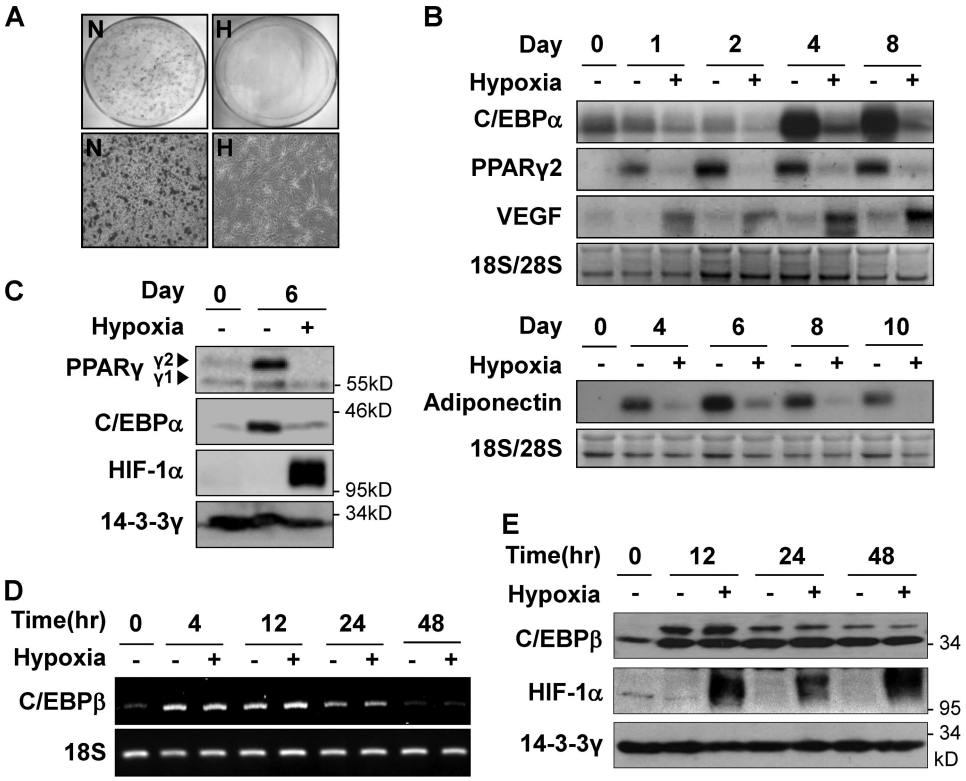

FIGURE 1. **Expression of PPARγ, C/EBPα, and C/EBPβ during adipogenesis.** Postconfluent 3T3-L1 cells were induced to differentiate by treatment with adipogenesis-inducing hormones under normoxic (20% O_2) or hypoxic (1% O_2) conditions for the indicated periods of time. *A*, after 8 days, cells were stained with Oil Red O. *N*, normoxia; *H*, hypoxia. *B*, total RNA isolated from the hormone-treated 3T3-L1 cells. Northern analysis was performed to detect PPARγ2, C/EBPα, vascular endothelial growth factor (*VEGF*), and adiponectin mRNA. 18 S/28 S rRNA was used as a loading control. *C*, Western analysis was performed with anti-PPARγ, anti-C/EBPα, anti-HIF-1α, and 14-3-3γ antibodies. 14-3-3γ protein served as a loading control. *D*, reverse transcription-PCR was performed using primers specific for C/EBPβ and 18 S rRNA. *E*, Western analysis was performed with anti-C/EBPβ, anti-HIF-1α, and anti-14-3-3γ antibodies. Two active isoforms of C/EBPβ (38 and 34-kDa) were detected. 14-3-3γ protein served as a loading control.

assay showed a reduction in the number of nuclear proteins bound to probes containing C/EBP binding sites (supplemental Fig. 1*A*).

As preadipocytes enter S-phase, C/EBPβ acquires DNA binding ability and localizes to centromeres by binding to C/EBP consensus-binding sites within centromeric satellite DNA. By binding to centromeric DNA, C/EBPβ becomes associated with punctate nuclear components (19). Consistent with this, immunofluorescence revealed that 20 h after hormone induction, C/EBPβ formed a punctate pattern, demonstrating that C/EBPβ binds to pericentromeric satellite DNA as preadipocytes enter S-phase (Fig. 2*D*) (18, 26). In contrast, C/EBPβ was distributed diffusely within nuclei 4 h post-treatment. This diffuse staining pattern was also observed even at 20 h after induction under hypoxic conditions. These findings indicate that hypoxia prevents C/EBPβ DNA binding during adipocyte differentiation.

We also tested the expression level of C/EBPδ, the other early induced C/EBP family during adipogenesis, and its localization in hypoxic conditions. Hypoxia does not affect C/EBPδ expression and localization (data not shown). The C/EBP homologue CHOP10, also known as GADD153 or C/EBPζ, inhibits the DNA binding capacity of C/EBPβ through heterodimerization with the factor. The expression level of CHOP10 correlates inversely with adipogenesis (27). Reports have demonstrated that anoxia (0% O_2) and endoplasmic reticulum stress increase CHOP10 expression (28). Western analysis revealed that CHOP10 levels decrease, whereas that of C/EBPβ increases (Fig. 2*E*). However, hypoxic treatment did not affect CHOP10 protein levels during adipogenesis, suggesting that the inability of C/EBPβ to bind DNA is not due to an increase in CHOP10 during hypoxia.

Hypoxia Blocks the Mitotic Clonal Expansion (MCE) of Preadipocytes—Although C/EBPβ gains its DNA binding ability as preadipocytes progress through the G_1/S transition, the cause-and-effect relationship between these two events is unclear. FACS analyses showed that 3T3-L1 cells undergo the G_1/S transition 12–18 h after induction. However, hypoxia leads to G_1-phase arrest (Fig. 3*A*). Cell-to-cell contact in confluent 3T3-L1 cells abrogates cell cycle progression by inducing the cyclin-dependent kinase inhibitor $p27^{Kip1}$, which suppresses the activity of CDK4 (cyclin-dependent kinase 4). CDK4 phosphorylates Rb, which is a prerequisite for the G_1/S transition. In early G_1, corresponding to 1–4 h postinduction (Fig. 3*B*), $p27^{Kip1}$ protein is detected, and Rb is hypophosphorylated (29). However, 12–24 h after induction, $p27^{Kip1}$ is diminished, leading to phosphorylation of Rb and resumption of the cell cycle (30, 31). In contrast, under hypoxic conditions, $p27^{Kip1}$ levels remain high because this protein is induced by HIF-1α (32) (see also Fig. 3*B*). Thus, hypoxia maintains $p27^{Kip1}$ at high levels, keeping Rb hypophosphorylated regardless of adipogenesis-inducing hormone treatment (MDI) (Fig. 3*B*) (33).

Based on these findings, we hypothesized that hypoxia blocks the G_1/S transition, thereby preventing C/EBPβ from acquiring the ability to bind DNA (32–34). Therefore, we tested whether HIF-1α-dependent induction of $p27^{Kip1}$ could prevent both the G_1/S transition and C/EBPβ activation. 3T3-L1 cells infected with retroviruses encoding $p27^{Kip1}$ were used. Moreover, constitutive expression of $p27^{Kip1}$ inhibited PPARγ and C/EBPα induction and adipogenesis even upon exposure to adipogenesis-inducing hormones (Fig. 3*C*). FACS and Western analyses revealed that the presence of $p27^{Kip1}$ was sufficient to block both Rb phosphorylation and the G_1/S transition (Fig. 3, *D* and *E*) (35, 36). Immunofluorescence analyses showed that $p27^{Kip1}$ can prevent C/EBPβ from acquiring DNA binding ability even under normoxia (Fig. 3*F*). These results suggest that hypoxia-induced HIF-1α maintains $p27^{Kip1}$ at a sufficiently high level to

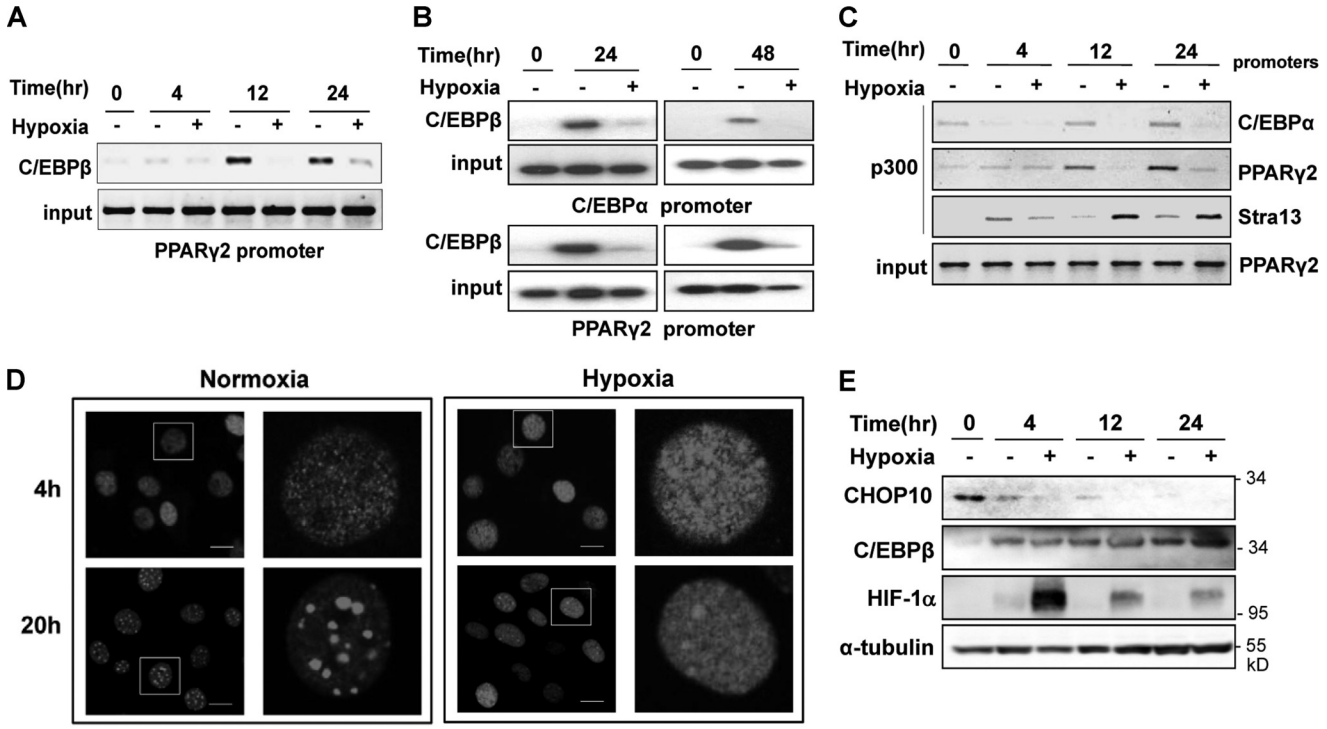

FIGURE 2. **DNA binding activity and heterochromatin localization of C/EBPβ.** Postconfluent 3T3-L1 cells were treated with MDI for the indicated times and then fixed and harvested for ChIP analysis. *A*, ChIP analysis of C/EBPβ binding to the PPARγ2 promoter *in vivo*. Using anti-C/EBPβ antibody, protein-genomic DNA complexes were immunoprecipitated (*IP*) and analyzed by 30 cycles of PCR. *Input* indicates that PCR was performed using 10% of the amount of sonicated cell lysate that was used for immunoprecipitation. *B*, using anti-C/EBPβ antibody, protein-genomic DNA complexes were immunoprecipitated and analyzed by 22 cycles of PCR. PCR was performed in the presence of [α-^{32}P]dATP and primers for C/EBPα (*top*) or the PPARγ2 promoter (*bottom*). *C*, ChIP analysis of p300 binding to the promoters of C/EBPα (*top*), PPARγ2 (*middle*), and Stra13 (*bottom*) *in vivo*. *D*, confocal microscopic images of C/EBPβ in differentiating 3T3-L1 cells. One cell in a *white square* was magnified and shown on the *right*. *E*, Western analysis of treated 3T3-L1 cells using anti-CHOP10, anti-C/EBPβ, anti-HIF-1α, and anti-α-tubulin antibodies. α-Tubulin was used as a loading control.

block mitotic clonal expansion, thus preventing C/EBPβ activation. Therefore, hypoxia can block 3T3-L1 cell adipogenesis by promoting HIF-1α-dependent induction of p27^{Kip1}.

G_1/S Transition Does Not Occur in Hypoxic HIF-1α Knockdown 3T3-L1 Cells—We further investigated whether HIF-1α is indispensable for hypoxic inhibition of C/EBPβ DNA binding ability. To perform these experiments, HIF-1α-deficient 3T3-L1 cells were generated by retroviral infection of shRNA specific against mouse HIF-1α. HIF-1α was stable during hypoxia in 3T3-L1 cells infected with retrovirus encoding control shRNA but not HIF-1α shRNA (Fig. 4*A*). Moreover, hypoxia induced p27^{Kip1} in 3T3-L1 cells infected with control shRNA but not in HIF-1α shRNA. This is consistent with a previous report showing the failure of hypoxia to induce p27^{Kip1} in HIF-1α knock-out mouse embryonic fibroblasts (32). Nonetheless, Rb was not phosphorylated under hypoxic conditions even in 3T3-L1 cells where neither HIF-1α nor p27^{Kip1} was induced (Fig. 4*A*, *lanes 8* and *10*, and supplemental Fig. 2*A*). FACS analyses showed that hypoxia arrests HIF-1α knockdown 3T3-L1 cells at G_1-phase, similar to control cells (Fig. 4*B*). These findings suggest that hypoxia inhibits Rb phosphorylation and G_1/S transition in the absence of p27^{Kip1} in differentiating 3T3-L1 cells. Gardner *et al.* (33) demonstrated that, in p27^{Kip1}-deficient murine fibroblast cells, hypoxia neither inhibits Rb phosphorylation nor causes G_1-phase arrest, indicating that HIF-1α induction of p27^{Kip1} is the primary pathway by which Rb hypophosphorylation and G_1 arrest occur in response to hypoxia. However, this pathway is not unique to differentiating 3T3-L1 cells. Our results indicate that hypoxia can block the G_1/S transition and Rb phosphorylation in a HIF-1α-independent manner, especially in differentiating 3T3-L1 cells.

Furthermore, induction of PPARγ and C/EBPα and lipid droplet formation in response to adipogenesis-inducing hormones during normoxia were unaffected by HIF-1α knockdown (Fig. 5, *A* and *B*). These findings confirmed that infected preadipocytes retain their ability to differentiate into mature adipocytes regardless of the presence of HIF-1α. In contrast, hypoxia blocks hormonal induction of PPARγ and C/EBPα and lipid droplet formation in the absence of HIF-1α (Fig. 5, *A* and *B*). ChIP analyses further verified these results because C/EBPβ binding to the PPARγ2 and C/EBPα promoters was abrogated by hypoxia even in 3T3-L1 cells lacking HIF-1α (Fig. 5*C*). Immunofluorescence demonstrated that hypoxia prevents C/EBPβ from acquiring a punctate pattern in these cells (Fig. 5*D*). These findings indicated that hypoxia prevented C/EBPβ from acquiring DNA binding ability not only by HIF-1α-dependent induction of p27^{Kip1} but also by a HIF-1α-independent pathway.

Dual Phosphorylation of C/EBPβ by both ERK and GSK3β—Recent studies have suggested that dual phosphorylation of C/EBPβ is required for this factor to acquire DNA binding ability (16, 17, 37). Both ERK, which is activated early in the G_1-phase, and CDK2/cyclin A, which is activated at the G_1/S

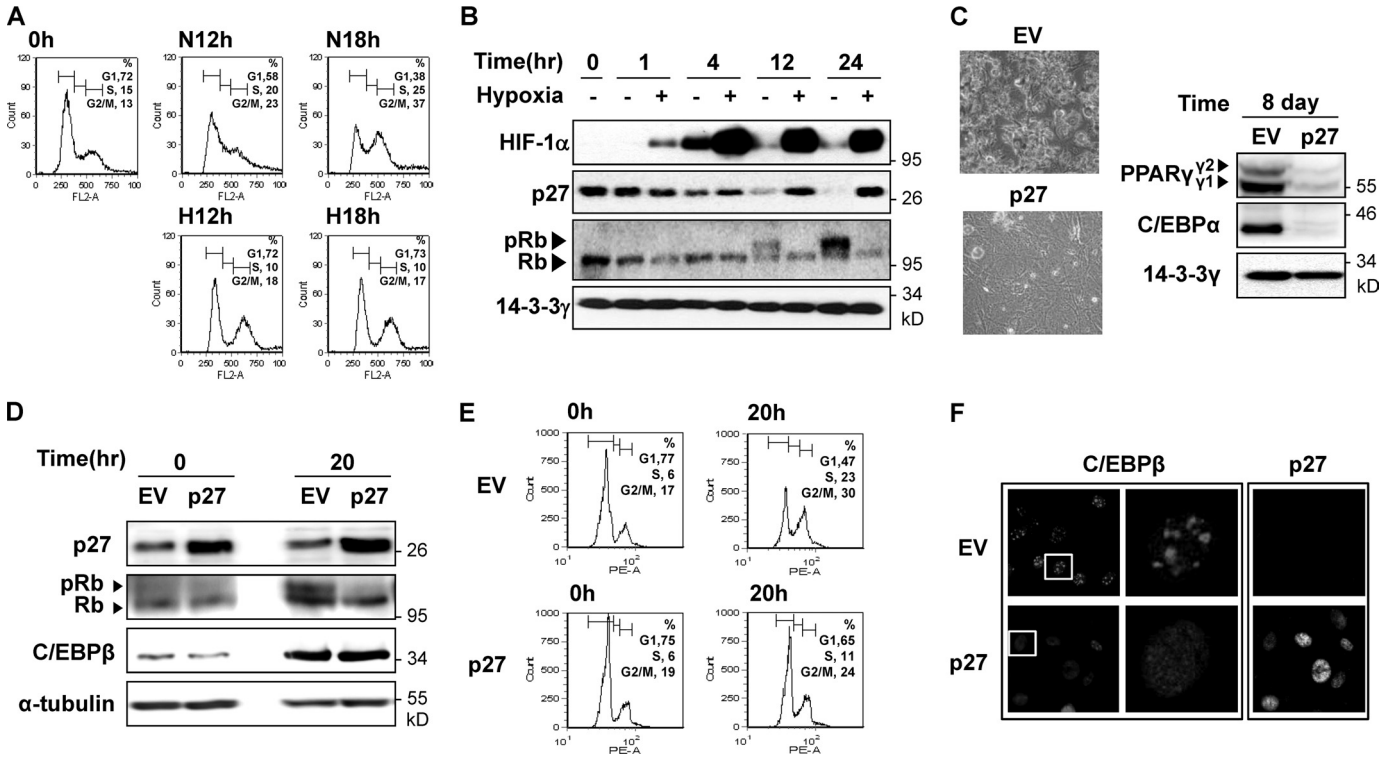

FIGURE 3. **Mitotic clonal expansion of 3T3-L1 cells during adipogenesis.** Postconfluent 3T3-L1 cells were induced to differentiate by treatment with MDI under normoxic or hypoxic conditions. *A*, flow cytometry of cells under normoxic (*N*) and hypoxic (*H*) conditions. *B*, Western analysis of treated 3T3-L1 cells was performed with anti-Rb, anti-p27, and anti-14-3-3γ-antibodies. 14-3-3γ was used as a loading control. *C*, effects of retroviral expression of $p27^{Kip1}$ in 3T3-L1 cells. As a control, 3T3-L1 cells were infected with retrovirus encoding an empty vector (*EV*). The selected 3T3-L1 cells were treated with MDI. Eight days after differentiation, 3T3-L1 cells were stained with Oil Red O as described. The levels of PPARγ and C/EBPα protein were determined by Western analysis. 14-3-3γ was used as a loading control. *D*, the selected 3T3-L1 cells were treated with MDI for 20 h under normoxia. The protein levels of p27, C/EBPβ, and Rb were determined by Western blot. *E*, the selected 3T3-L1 cells were induced to differentiate for the indicated times, fixed with 70% ethanol, and stained with PI. The PI-stained cells were analyzed by flow cytometry. *F*, confocal microscopic images of C/EBPβ in differentiating 3T3-L1 cells. The infected 3T3-L1 cells were treated with MDI for 20 h under normoxia. The stained C/EBPβ in 3T3-L1 cells was observed with a Zeiss LSM510 inverted confocal microscope. One cell in a *white square* was magnified and shown on the *right*.

transition, maintain C/EBPβ phosphorylation at Thr^{188} throughout the G_1 and S phases. Phosphorylation of this residue is required for subsequent phosphorylation of Thr^{179} or Ser^{184} by GSK3β (16). By using *in vitro* phosphorylation of C/EBPβ and an electrophoretic mobility shift assay, we confirmed that both ERK and GSK3β are required for the dual phosphorylation of C/EBPβ and acquisition of its DNA binding ability (supplemental Fig. 1, *B* and *C*). To determine whether hypoxia blocks this sequential process, we investigated ERK activation by Western blot analysis. The level of phosphorylated ERK increased within 1 h of induction and diminished within 12 h. ERK remained phosphorylated even under hypoxic conditions (Fig. 6*A*). Therefore, hypoxia does not block the activation of ERK. Western blot analysis of C/EBPβ showed that Thr^{188} phosphorylation was sustained 12–24 h after induction (Fig. 6*B*). This antibody specifically recognizes phosphorylated Thr^{188} on C/EBPβ (supplemental Fig. 1*D*) (17). These data indicate that Thr^{188} is not involved in the inability of C/EBPβ to bind DNA during hypoxia.

As adipogenesis proceeds, the amount of GSK3β in the nucleus increases gradually before terminal differentiation. Tang *et al.* suggested that, during the G_1/S transition, GSK3β translocates into the nucleus, where it phosphorylates other nuclear proteins, including C/EBPβ and cyclin D1 (31, 38). Our data demonstrate that hypoxia blocks GSK3β nuclear translocation during adipogenesis (Fig. 6*C*), thereby preventing phosphorylation of C/EBPβ at Thr^{179} and/or Ser^{184}. In addition, immunoblotting using an antibody specific for phosphorylated Ser^9 of GSK3β revealed that hypoxia increases the level of inactive GSK3β (Fig. 6*D*).

The Role of GSK3β and ERK in C/EBPβ DNA Binding—We further investigated the biochemical mechanism involved in hypoxia-induced inhibition of C/EBPβ DNA binding. Immunofluorescence showed that treatment of cells with the GSK3β inhibitors LiCl and 6-bromoindirubin-3′-oxime (BIO) for 8 or 20 h before harvest abrogated the punctate distribution of C/EBPβ (Fig. 7*A*). Likewise, treatment with U0126, an inhibitor of mitogen-activated protein kinase/extracellular signal-regulated kinase kinase (MEK), the upstream kinase of ERK, for 20 or 12 h (*20 h* and *Early 12 h* indicated in Fig. 7) at the beginning of MDI treatment produced the same effect. Later exposures (*i.e.* 2 and 8 h (*Late 2 h* and *Late 8 h* indicated in Fig. 7)) of U0126 produced a punctate staining pattern, confirming that ERK is activated only during early G_1-phase, which occurs ~1–12 h after MDI treatment (Fig. 6*A*). Moreover, shorter exposures of hypoxia or the GSK3β inhibitors for 2 h (*Late 2 h* indicated in Fig. 7) at the end of MDI treatment also yielded a punctate C/EBPβ distribution, indicating that GSK3β activity is required during the G_1/S transition, which occurs approximately 12–18 h after MDI treatment. The results from ChIP analyses shown in Fig. 7*B* confirm

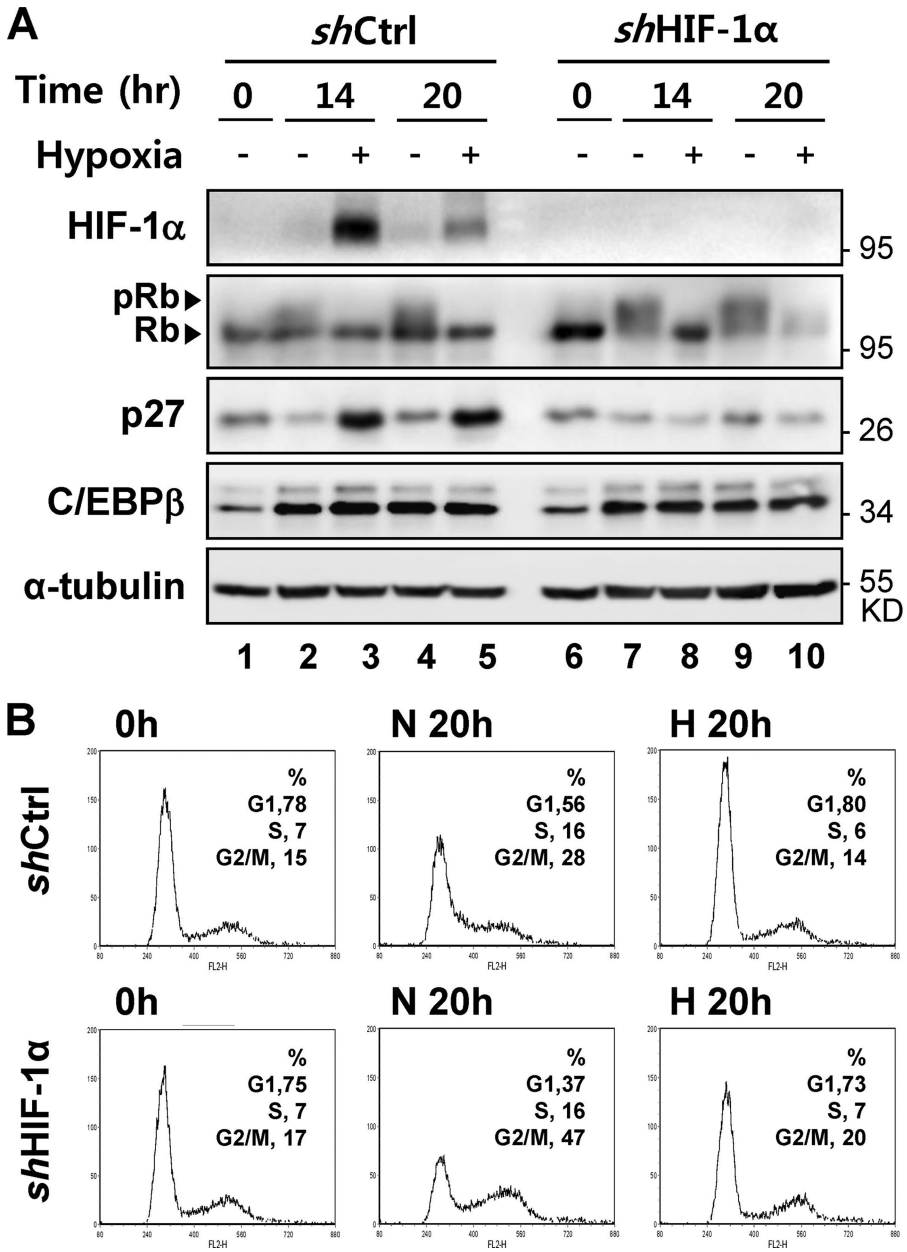

FIGURE 4. **Effect of HIF-1α knockdown on G_1/S transition during adipogenesis.** Preadipocyte 3T3-L1 cells were infected with retrovirus encoding control shRNA (*sh*Ctrl) or shRNAs against mouse HIF-1α (*sh*HIF-1α). Cells were induced to differentiate by treatment with MDI under normoxia or hypoxia for the indicated times. *A*, Western blot analysis was performed with anti-Rb, anti-p27, anti-HIF-1α, anti-C/EBPβ, and anti-α-tubulin antibodies. Two active isoforms of C/EBPβ (38 and 34 kDa) were detected. α-Tubulin was used as a loading control. *B*, at the indicated times after hormone induction, 3T3-L1 cells were trypsinized, fixed with 70% ethanol, stained with PI, and analyzed by flow cytometry. *N*, normoxia; *H*, hypoxia.

that both U0126 and BIO prevent C/EBPβ binding to the promoters of C/EBPα and PPARγ2, suggesting that ERK and GSK-3β are required for C/EBPβ to acquire its DNA binding ability.

GSK-3β also phosphorylates β-catenin, leading to its degradation. We confirmed that LiCl and BIO treatment increased β-catenin nuclear translocation by blocking GSK-3β activity. MDI treatment causes GSK-3β levels to increase within the nucleus and β-catenin to decrease. However, during hypoxia, GSK-3β levels within the nucleus did not increase, allowing β-catenin levels to also remain unaffected in MDI-treated 3T3-L1 cells (Fig. 7*C*). The finding that Wnt inhibits adipogenesis via the β-catenin/T-cell factor (Tcf)-dependent pathway suggests that, during hypoxia, increased levels of β-catenin contribute to the hypoxic repression of PPARγ2 (39). Different from hypoxia, GSK3β inhibitors did not induce p27. Thus, Rb remains phosphorylated in MDI-treated 3T3-L1 cells, even in the presence of either LiCl or BIO. These results indicated that GSK3β activity is not required for Rb phosphorylation (Fig. 7*D*). Moreover, we discovered that constitutive expression of p27 in 3T3-L1 cells prevented GSK3β nuclear translocation in response to adipogenesis-inducing hormones even under normoxia (Fig. 8*A*), suggesting that Rb phosphorylation and the G_1/S transition cause GSK3β translocation into the nucleus.

We also investigated whether HIF-1α is involved in the hypoxic inhibition of GSK3β nuclear translocalization. Hypoxia still prevents GSK-3β nuclear translocation in HIF-1α knockdown 3T3-L1 cells (Fig. 8*B*). These results imply that hypoxia blocks GSK-3β nuclear localization by a HIF-1α-independent mechanism. Collectively, our results demonstrated that hypoxia inhibits C/EBPβ activation by blocking the nuclear localization of GSK3β via an HIF-1α-independent and HIF-1α/p27-dependent mechanisms.

DISCUSSION

Because C/EBPβ is sequentially phosphorylated during the G_1 and S phases, other check points for mitosis are also expected to regulate the dual phosphorylation of C/EBPβ. Protein kinases that catalyze the phosphorylation of C/EBPβ are tightly regulated by the cell cycle. ERK, CDK2/cyclin A, and GSK3β are activated during G_1 and the G_1/S transition. GSK3β is localized predominantly within the cytoplasm during early G_1-phase (2–8 h), but a significant fraction of GSK3β translocates to the nucleus during the G1/S transition (Fig. 6*C*). Because Thr^{188} of C/EBβ remained phosphorylated even during hypoxia, hypoxia inhibits the DNA binding ability of C/EBPβ by a mechanism that does not involve this residue. Results from this study suggest that hypoxia prevents C/EBPβ from acquiring DNA binding ability by blocking GSK3β nuclear translocation. Our findings that (i) GSK3β failed to translocate into the nucleus when Rb was hypophos-

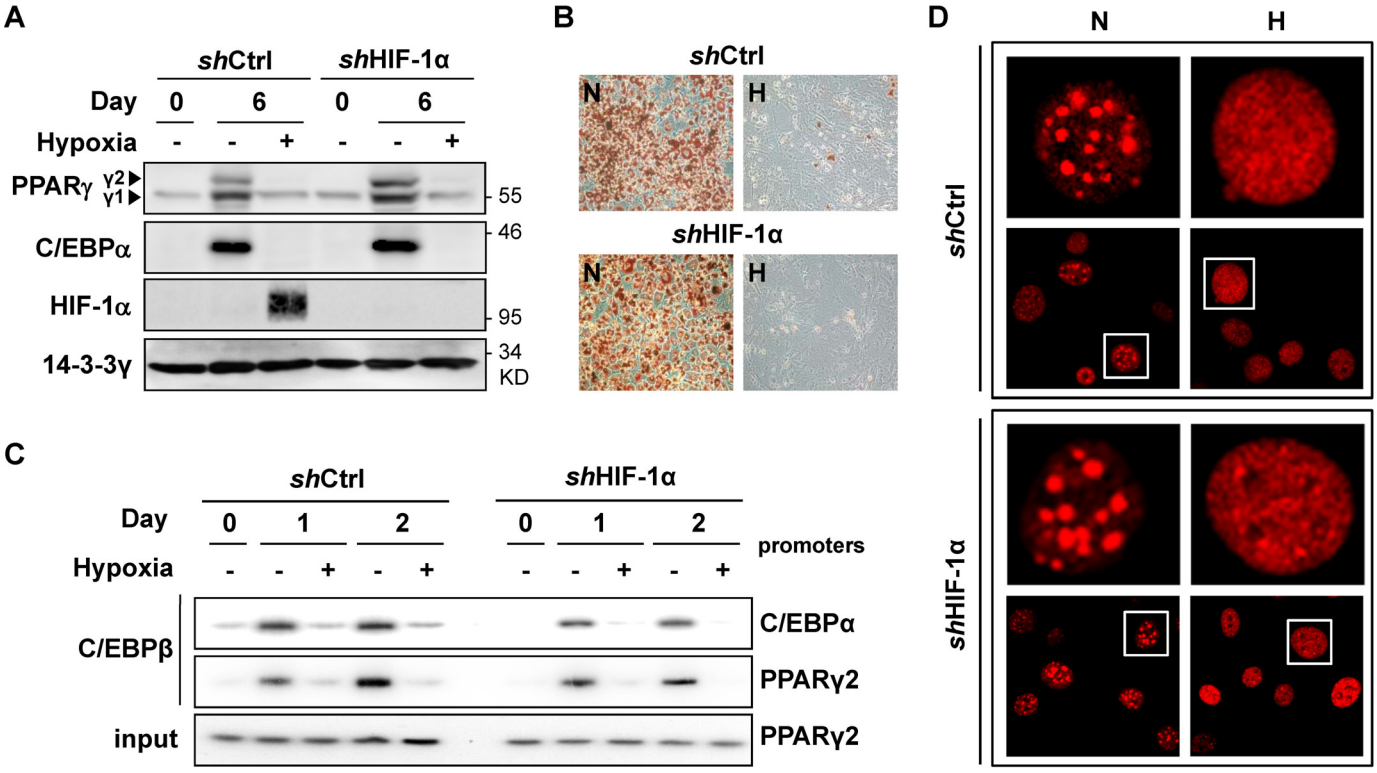

FIGURE 5. **Effect of HIF-1α knockdown on the DNA binding ability of C/EBPβ during adipogenesis.** *A*, after a 6-day treatment with MDI, Western analysis was performed using anti-PPARγ, anti-C/EBPα, anti-HIF-1α, and anti-14-3-3γ antibodies. 14-3-3γ was used as a loading control. *B*, after 8 days, 3T3-L1 cells were stained with Oil Red O. *C*, hormone-treated 3T3-L1 cells were fixed and harvested for ChIP analysis using primers against the PPARγ2 and C/EBPα promoters. *Input* indicates that PCR was performed using 10% the amount of sonicated cell lysate that was used for immunoprecipitation (*IP*). *D*, 3T3-L1 cells were carried out on glass coverslips and differentiated for 20 h under normoxic or hypoxic conditions. Confocal microscopic images of cellular C/EBPβ were observed using a Zeiss LSM510 microscope. One cell in a *white square* was magnified and shown in the *upper panel*. *N*, normoxia; *H*, hypoxia.

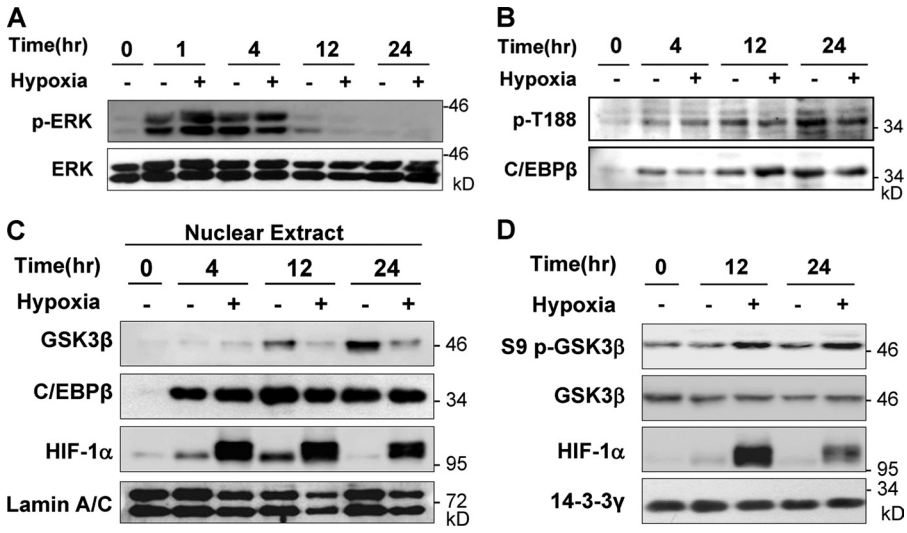

FIGURE 6. **Phosphorylation of C/EBPβ, ERK and GSK3β.** Postconfluent 3T3-L1 cells were induced to differentiate by treatment with MDI under normoxic (20% O_2) or hypoxic (1% O_2) conditions for the indicated periods of time. Whole cell extracts of the treated 3T3-L1 cells were subjected to Western blot analysis using anti-phospho-ERK (*top*) or anti-ERK antibodies (*bottom*) (*A*) or anti-Thr^{188} phospho-C/EBPβ (*top*) or anti-C/EBPβ antibodies (*bottom*) (*B*). *C*, nuclear extracts were prepared from the hormone-treated 3T3-L1 cells as described under "Experimental Procedures." Using 10 μg of nuclear extracts, Western analysis was performed with anti-GSK3β, anti-C/EBPβ, anti-HIF-1α, or anti-lamin A/C antibodies. Lamin A/C was used as a loading control for the nuclear extracts. *D*, Western analysis on whole cell extracts was performed using anti-phospho-Ser^{9}-GSK3β, anti-GSK3β, anti-HIF-1α, or anti-14-3-3γ antibodies. 14-3-3γ was used as a loading control.

phorylated and when 3T3-L1 cells were arrested at G_1-phase and (ii) GSK3β inhibitors did not block Rb phosphorylation imply that hypoxia blocks nuclear translocation of GSK3β by blocking G_1/S transition but not that hypoxic inhibition of GSK3β nuclear translocation causes hypophosphorylation of Rb and G_1 arrest. However, it is still unclear how GSK3β acquires the ability to enter the nucleus during the G_1/S transition. Further investigation is necessary to examine the possibility that hypoxia directly inhibits GSK3β nuclear translocation.

Hypoxia prevents most cells from traversing the G_1/S checkpoint through hypophosphorylation of the Rb protein by inducing p27^{Kip1} in a HIF-1α-dependent manner. Goda *et al.* (32) demonstrated that in murine embryonic fibroblasts (MEFs) and splenic B lymphocytes deficient in HIF-1α, hypoxia fails to block the G_1/S transition and Rb phosphorylation, suggesting that HIF-1α is indispensable for these events. Gardner *et al.* demonstrated that in p27^{Kip1}-deficient MEFs, hypoxia neither inhibits Rb phosphorylation nor causes G_1 arrest. However, in p21^{Cip1}-deficient MEFs, hypoxia causes the fibroblasts to arrest in the G_1-phase

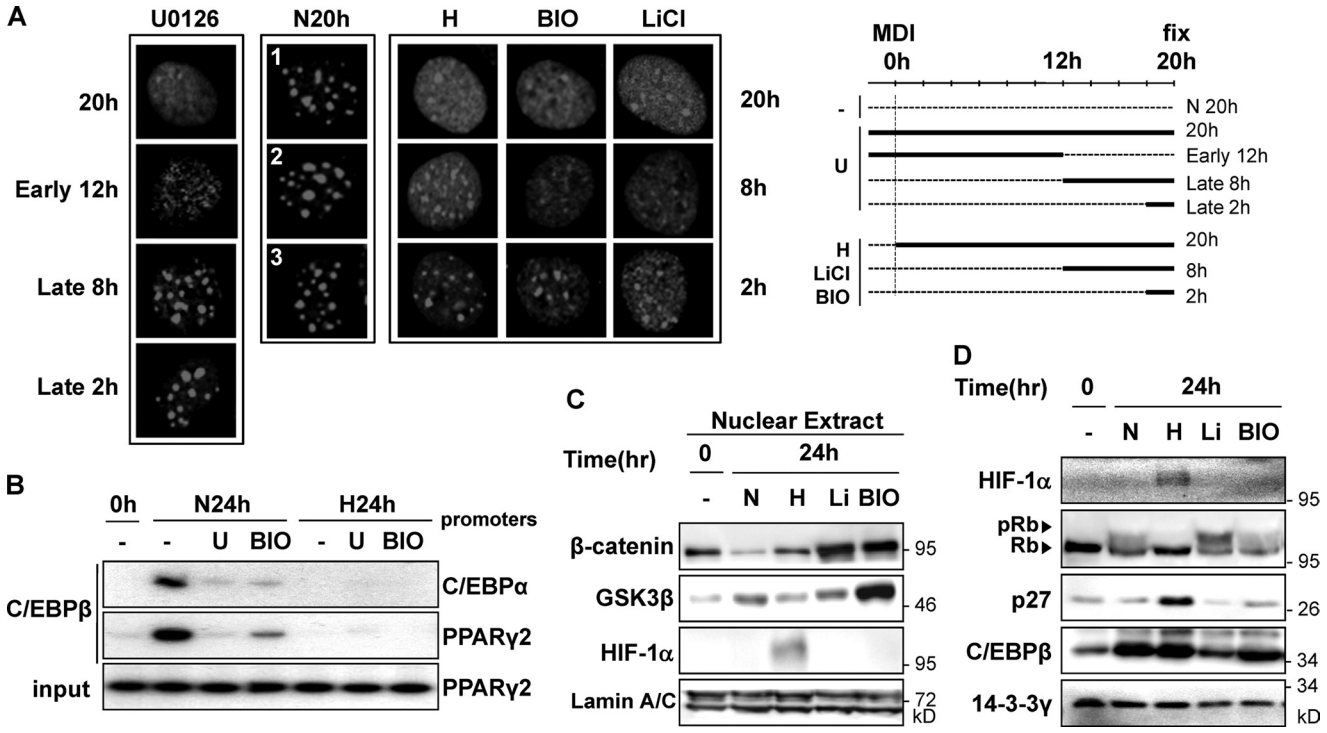

FIGURE 7. **DNA binding activity and heterochromatin localization of C/EBPβ in the presence of inhibitors.** *A*, 3T3-L1 cells were cultured on glass coverslips and induced to differentiate by treatment with MDI for 20 h. Three different differentiating cells (*1–3*) are shown under normoxia (*N20h*). The differentiating cells were treated with U0126 (20 μM), BIO (1 μM), or LiCl (20 mM) for the indicated times (marked with *heavy black bars* in the *right panel*) under normoxic conditions. The cells were also exposed to hypoxia for the indicated times. Confocal microscopic images of cellular C/EBPβ were observed using a Zeiss LSM510 microscope. *N*, normoxia; *H*, hypoxia. *B*, in the presence of U0126 (*U*) (20 μM), BIO (1 μM), or DMSO (−) (0.1%, v/v), the postconfluent 3T3-L1 cells were induced to differentiate by treatment with MDI for 24 h. The treated 3T3-L1 cells were then fixed and harvested for ChIP analyses using an anti-C/EBPβ antibody and primers against the C/EBPα (*top*) and PPARγ2 promoters (*bottom*). *Input* indicates that PCR was performed using 10% of the amount of sonicated cell lysate that was used for immunoprecipitation. *C*, postconfluent 3T3-L1 cells were treated with MDI for 24 h in the presence of LiCl (20 mM) and BIO (1 μM) or under hypoxic conditions. Using 10 μg of the nuclear extracts of the treated 3T3-L1 cells, Western analysis was performed with anti-β-catenin, anti-GSK3β, anti-HIF-1α, and anti-lamin A/C antibodies. Lamin A/C was used as a loading control for the nuclear extracts. *D*, Western analysis on whole cell extracts of the treated 3T3-L1 cells was performed using anti-p27, anti-Rb, anti-HIF-1α, anti-C/EBPβ, and anti-14-3-3γ antibodies. 14-3-3γ was used as a loading control.

(33). These findings suggest that HIF-1α-induced $p27^{Kip1}$ is a unique cell cycle inhibitor that mediates Rb hypophosphorylation and G_1 arrest in fibroblasts in response to hypoxic stress. Consistent with this, we observed that $p27^{Kip1}$, but not $p21^{Cip1}$, was induced by hypoxia in 3T3-L1 cells (supplemental Fig. 2*B*). We also showed that 3T3-L1 lacking HIF-1α failed to induce $p27^{Kip1}$ in response to hypoxia. Nevertheless, in hypoxic HIF-1α-knockdown preadipocytes, Rb remained hypophosphorylated even in the absence of $p27^{Kip1}$ induction. This suggests that, particularly when under the control of adipogenesis-inducing hormones, hypoxia can block Rb phosphorylation by a mechanism distinct from the HIF-1α-dependent induction of $p27^{Kip1}$. By using monkey kidney epithelial cells, Krtolica *et al.* (40) showed that, in addition to increases in $p27^{Kip1}$, hypoxia lowers cyclin D and E protein levels and increases Rb-directed protein phosphatase 1, thus reducing cyclin-CDK activity. Green *et al.* (34) showed repression of CDK2 activity and Rb hypophosphorylation in hypoxic $p21^{Cip1}$- and $p27^{Kip1}$-deficient ($p21^{Cip1-/-}$, $p27^{Kip1-/-}$) MEFs, indicating that, without $p21^{Cip1}$ and $p27^{Kip1}$, hypoxia still inhibits CDK2 activity. Hypoxia is also known to repress *cdc25a*, another cell cycle gene encoding a tyrosine phosphatase that maintains CDK2 activity. However, HIF-1α alone fails to repress this gene (41). Taken together, these findings indicate that additional factors besides HIF-1α and $p27^{Kip1}$ are involved in hypoxia-induced cell cycle arrest. Additional studies are required to investigate whether HIF is involved in the hypoxic regulation of cyclins, protein phosphatase 1, and Cdc25a.

We also found that hypoxia increases levels of inactive GSK3β, which is phosphorylated on Ser^9 by the upstream kinase Akt (Fig. 6*D* and supplemental Fig. 2*C*). Therefore, hypoxia inhibits both the nuclear localization and activity of GSK3β in MDI-treated 3T3-L1 cells. Like other GSK3β inhibitors, such as LiCl and BIO, hypoxia also increases the level of nuclear β-catenin, a well known target of GSK3β (Fig. 7*C*). Both β-catenin and GSK3β form a complex in the cytoplasm with the common scaffold protein axin. GSK3β phosphorylates the closely associated β-catenin and triggers its degradation. In response to canonical Wnt signaling, the complex formed by GSK3β, β-catenin, axin, and the anaphase-promoting complex is dissociated. Under these conditions, phosphorylation of β-catenin by GSK3β is reduced, and β-catenin retains greater stability and translocates into the nucleus. Canonical Wnt ligands, such as Wnt10b and Wnt3a, are known to inhibit adipogenesis by repressing both C/EBPα and PPARγ by a β-catenin/Tcf-dependent mechanism (39, 42). A previous study using bipotential mesenchymal ST2 cells showed that Wnt signals do not alter C/EBPβ expression (43, 44). It remains to be determined, however, whether nuclear β-catenin is involved in inhibiting the DNA binding ability of C/EBPβ. Both

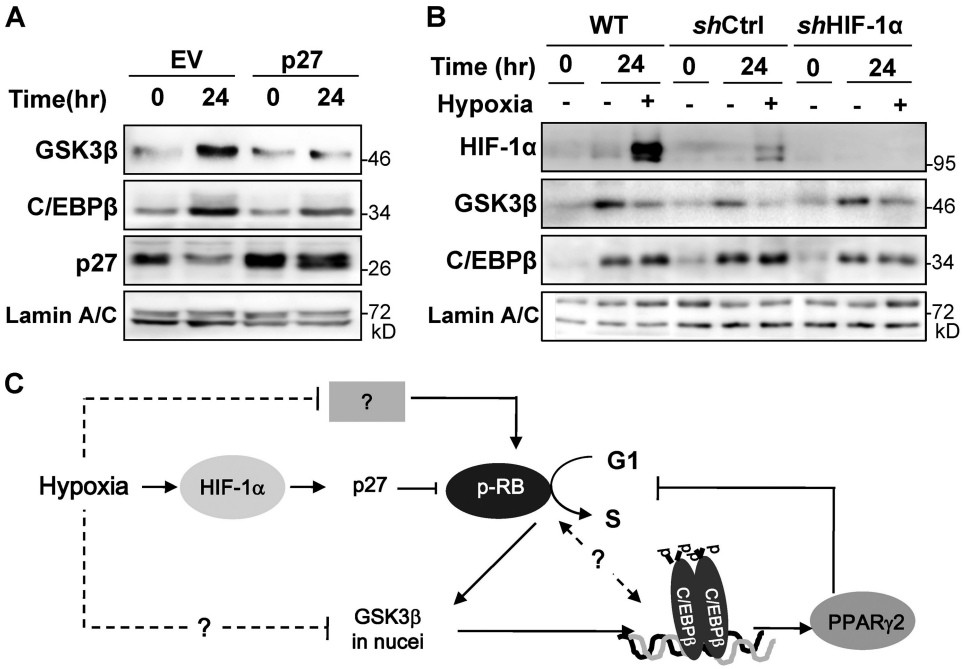

FIGURE 8. **Effect of HIF-1α and p27 on GSK-3β nuclear localization.** *A*, 3T3-L1 cells were infected with retrovirus encoding $p27^{Kip1}$. As a control, 3T3-L1 cells were infected with retrovirus carrying an empty vector (*EV*). The infected 3T3-L1 cells were treated with MDI for 24 h under normoxia. Nuclear extracts were isolated from the hormone-treated 3T3-L1 cells, and Western analysis was performed using anti-GSK3β, anti-C/EBPβ, anti-HIF-1α, or anti-lamin A/C antibodies. *B*, preadipocyte 3T3-L1 cells were infected with a retrovirus encoding control shRNA (*sh*Ctrl) or shRNAs against mouse HIF-1α (*sh*HIF-1α). The infected 3T3-L1 cells were induced to differentiate by treatment with MDI for 24 h under normoxic or hypoxic conditions for the indicated times. Nuclear extracts were isolated from the hormone-treated 3T3-L1 cells, and Western analysis was performed using anti-GSK3β, anti-C/EBPβ, anti-HIF-1α, or anti-lamin A/C antibodies. Lamin A/C was used as a loading control for the nuclear extracts. *C*, schematic diagram describing the HIF-1α-dependent and independent mechanisms of hypoxic inhibition of adipogenesis.

hypoxia and GSK3β inhibitors prevent C/EBPβ from binding to DNA. Unlike hypoxia, however, GSK3β inhibitors fail to inhibit the Rb phosphorylation (Fig. 7*D*). BIO and LiCl inhibited the catalytic activity of GSK3β, whereas hypoxia inhibited the nuclear localization and activity of GSK3β, presumably by blocking the G_1/S transition and activating the Akt pathway.

Because C/EBPβ activated in response to the G_1/S transition triggers the expression of PPARγ2, C/EBPβ can mediate signals from cell cycle events to transcriptional cascades, leading to irreversible terminal differentiation. The finding that a dominant negative C/EBPβ mutant, incapable of binding DNA, blocks MCE in 3T3-L1 preadipocytes suggests that the DNA binding ability of C/EBPβ is also required for proceeding through MCE followed by the G_1/S transition (19, 20). In addition, the fact that active C/EBPβ increases transcription of C/EBPα and PPARγ, which were also responsible for terminating MCE, implies that C/EBPβ is also responsible for halting MCE. Thus, C/EBPβ is involved in limiting MCE to one or two cell divisions prior to differentiation (19, 45, 46). Normal embryonic fibroblasts from lung buds differentiate into adipocytes in response to hormonal induction; however, embryonic fibroblasts deficient in Rb do not, indicating that Rb is essential for adipogenesis (47). The interaction between Rb and C/EBPβ occurred only in differentiating cells, and interaction with Rb appeared to inhibit the binding of C/EBPβ to cognate DNA sequences *in vitro* (48). Forced expression of C/EBPβ inhibited the proliferation of wild type MEFs but not of MEFs lacking all three Rb family proteins, suggesting that C/EBPβ represses genes required for cell cycle progression through interaction with Rb proteins (49). However, it remains to be determined how the phosphorylation states of both Rb and C/EBPβ affect these interactions.

Yun *et al.* (10) have demonstrated that the PPARγ2 promoter is suppressed by Stra13/DEC1, which is induced by HIF-1α, suggesting that HIF-1α and its target Stra13/DEC1 mediate hypoxic inhibition of adipogenesis after C/EBPβ-DNA interaction. Recently, Gulbagci *et al.* demonstrated that the Stra13/DEC1 isoform DEC2/SHARP1 interacts with C/EBPβ and enhances the recruitment of histone deacetylase 1 and histone methyltransferase G9a to the promoter of PPARγ2. Thus, DEC2/SHARP1 also represses adipogenesis (50). We demonstrated previously that both DEC1 and DEC2 repress the lipogenic transcription factor, SREBP-1c (sterol regulatory element binding protein-1c), by preventing binding to promoters of its targets, including the promoters of SREBP-1c and fatty acid synthase (24). These findings suggest that HIF-induced DEC1 and DEC2 are directly and indirectly involved in hypoxic inhibition of adipogenesis because SREBP-1c participates in the synthesis of a putative endogenous ligand for PPARγ during lipogenesis.

Hypoxia inhibits adipogenesis by blocking both the MCE and differentiation processes through (i) HIF-1-dependent induction of $p27^{Kip1}$ and (ii) HIF-1-independent inhibition of GSK3β and C/EBPβ signals (Fig. 8*C*). By recruiting such diverse pathways, preadipocytes can arrest adipogenesis any time oxygen is limited. This idea is consistent with fact that adipose tissue is a highly vascular connective tissue. Although hypoxia has an inhibitory effect on cell differentiation, hypoxia often promotes chondrogenesis of mesenchymal stem cells (51). Consistent with this, cartilage is known to be an avascular connective tissue. Recently, by analyzing HIF-1α-deficient mouse limbs, Amarilio *et al.* (52) showed that HIF-1α directly binds to and activates the promoter of *sox9*, a key transcription factor in chondrogenesis. Therefore, hypoxic conditions are necessary to promote the differentiation of prechondrocyte to chondrocytes (52). Stem cells and multipotent progenitor cells reside in complex microenvironments, or niches. During the early stages of development, the vasculature undergoes extensive remodeling. Specifically, oxygen gradients between blood vessels and stem cell niches might serve as important environmental cues to promote or inhibit differentiation, depending on the cell lineage involved (53). Our study provides insight into the role of oxygen, particularly in adipogenesis. Exposure of cells to

hypoxia at any stage of this process can inhibit the progress of adipogenesis by blocking many different checkpoints. Therefore, adipogenesis can proceed only when the vasculature can deliver sufficient oxygen and nutrients.

Acknowledgments—We thank Dr. Shizuo Akira, Dr. Robin Miskimins, Dr. Eui-Ju Choi, and Dr. Jae Bum Kim for providing cDNAs for C/EBPβ, p27, Rb, and PPARγ, respectively. We also thank Hyun-Ju Cho, Jieun Chung, and Heesang Cho for technical support.

REFERENCES

1. Sitkovsky, M., and Lukashev, D. (2005) *Nat. Rev. Immunol.* **5,** 712–721
2. Brahimi-Horn, M. C., and Pouyssegur, J. (2007) *FEBS Lett.* **581,** 3582–3591
3. Wouters, B. G., and Koritzinsky, M. (2008) *Nat. Rev. Cancer* **8,** 851–864
4. Jaakkola, P., Mole, D. R., Tian, Y. M., Wilson, M. I., Gielbert, J., Gaskell, S. J., Kriegsheim, A., Hebestreit, H. F., Mukherji, M., Schofield, C. J., Maxwell, P. H., Pugh, C. W., and Ratcliffe, P. J. (2001) *Science* **292,** 468–472
5. Lando, D., Peet, D. J., Gorman, J. J., Whelan, D. A., Whitelaw, M. L., and Bruick, R. K. (2002) *Genes Dev.* **16,** 1466–1471
6. Kaidi, A., Williams, A. C., and Paraskeva, C. (2007) *Nat. Cell Biol.* **9,** 210–217
7. Covello, K. L., Kehler, J., Yu, H., Gordan, J. D., Arsham, A. M., Hu, C. J., Labosky, P. A., Simon, M. C., and Keith, B. (2006) *Genes Dev.* **20,** 557–570
8. Takahashi, K., and Yamanaka, S. (2006) *Cell* **126,** 663–676
9. Gustafsson, M. V., Zheng, X., Pereira, T., Gradin, K., Jin, S., Lundkvist, J., Ruas, J. L., Poellinger, L., Lendahl, U., and Bondesson, M. (2005) *Dev. Cell* **9,** 617–628
10. Yun, Z., Maecker, H. L., Johnson, R. S., and Giaccia, A. J. (2002) *Dev. Cell* **2,** 331–341
11. Tang, Q. Q., Zhang, J. W., and Daniel Lane, M. (2004) *Biochem. Biophys. Res. Commun.* **318,** 213–218
12. Rosen, E. D., Walkey, C. J., Puigserver, P., and Spiegelman, B. M. (2000) *Genes Dev.* **14,** 1293–1307
13. Ramji, D. P., and Foka, P. (2002) *Biochem. J.* **365,** 561–575
14. Fajas, L., Fruchart, J. C., and Auwerx, J. (1998) *Curr. Opin. Cell Biol.* **10,** 165–173
15. Lane, M. D., Tang, Q. Q., and Jiang, M. S. (1999) *Biochem. Biophys. Res. Commun.* **266,** 677–683
16. Tang, Q. Q., Gronborg, M., Huang, H., Kim, J. W., Otto, T. C., Pandey, A., and Lane, M. D. (2005) *Proc. Natl. Acad. Sci. U.S.A.* **102,** 9766–9771
17. Li, X., Kim, J. W., Gronborg, M., Urlaub, H., Lane, M. D., and Tang, Q. Q. (2007) *Proc. Natl. Acad. Sci. U.S.A.* **104,** 11597–11602
18. Tang, Q. Q., and Lane, M. D. (1999) *Genes Dev.* **13,** 2231–2241
19. Tang, Q. Q., Otto, T. C., and Lane, M. D. (2003) *Proc. Natl. Acad. Sci. U.S.A.* **100,** 850–855
20. Zhang, J. W., Tang, Q. Q., Vinson, C., and Lane, M. D. (2004) *Proc. Natl. Acad. Sci. U.S.A.* **101,** 43–47
21. Ko, H. P., Okino, S. T., Ma, Q., and Whitlock, J. P., Jr. (1996) *Mol. Cell. Biol.* **16,** 430–436
22. Yim, S., Oh, M., Choi, S. M., and Park, H. (2004) *Biochem. Biophys. Res. Commun.* **322,** 9–16
23. Choi, S. M., Choi, K. O., Park, Y. K., Cho, H., Yang, E. G., and Park, H. (2006) *J. Biol. Chem.* **281,** 34056–34063
24. Choi, S. M., Cho, H. J., Cho, H., Kim, K. H., Kim, J. B., and Park, H. (2008) *Nucleic Acids Res.* **36,** 6372–6385
25. Park, S. K., Oh, S. Y., Lee, M. Y., Yoon, S., Kim, K. S., and Kim, J. W. (2004) *Diabetes* **53,** 2757–2766
26. Piwien Pilipuk, G., Galigniana, M. D., and Schwartz, J. (2003) *J. Biol. Chem.* **278,** 35668–35677
27. Tang, Q. Q., and Lane, M. D. (2000) *Proc. Natl. Acad. Sci. U.S.A.* **97,** 12446–12450
28. Carriere, A., Carmona, M. C., Fernandez, Y., Rigoulet, M., Wenger, R. H., Penicaud, L., and Casteilla, L. (2004) *J. Biol. Chem.* **279,** 40462–40469
29. Olashaw, N., and Pledger, W. J. (2002) *Sci. STKE 2002*, RE7
30. Patel, Y. M., and Lane, M. D. (2000) *J. Biol. Chem.* **275,** 17653–17660
31. Tang, Q. Q., Otto, T. C., and Lane, M. D. (2003) *Proc. Natl. Acad. Sci. U.S.A.* **100,** 44–49
32. Goda, N., Ryan, H. E., Khadivi, B., McNulty, W., Rickert, R. C., and Johnson, R. S. (2003) *Mol. Cell. Biol.* **23,** 359–369
33. Gardner, L. B., Li, Q., Park, M. S., Flanagan, W. M., Semenza, G. L., and Dang, C. V. (2001) *J. Biol. Chem.* **276,** 7919–7926
34. Green, S. L., Freiberg, R. A., and Giaccia, A. J. (2001) *Mol. Cell. Biol.* **21,** 1196–1206
35. Hackenbeck, T., Knaup, K. X., Schietke, R., Schodel, J., Willam, C., Wu, X., Warnecke, C., Eckardt, K. U., and Wiesener, M. S. (2009) *Cell Cycle* **8,** 1386–1395
36. Okada, M., Sakai, T., Nakamura, T., Tamamori-Adachi, M., Kitajima, S., Matsuki, Y., Watanabe, E., Hiramatsu, R., Sakaue, H., and Kasuga, M. (2009) *Biochem. Biophys. Res. Commun.* **379,** 249–254
37. Kim, J. W., Tang, Q. Q., Li, X., and Lane, M. D. (2007) *Proc. Natl. Acad. Sci. U.S.A.* **104,** 1800–1804
38. Diehl, J. A., Cheng, M., Roussel, M. F., and Sherr, C. J. (1998) *Genes Dev.* **12,** 3499–3511
39. Liu, J., Wang, H., Zuo, Y., and Farmer, S. R. (2006) *Mol. Cell. Biol.* **26,** 5827–5837
40. Krtolica, A., Krucher, N. A., and Ludlow, J. W. (1998) *Oncogene* **17,** 2295–2304
41. Hammer, S., To, K. K., Yoo, Y. G., Koshiji, M., and Huang, L. E. (2007) *Cell Cycle* **6,** 1919–1926
42. Ross, S. E., Hemati, N., Longo, K. A., Bennett, C. N., Lucas, P. C., Erickson, R. L., and MacDougald, O. A. (2000) *Science* **289,** 950–953
43. Prestwich, T. C., and Macdougald, O. A. (2007) *Curr. Opin. Cell Biol.* **19,** 612–617
44. Kang, S., Bennett, C. N., Gerin, I., Rapp, L. A., Hankenson, K. D., and Macdougald, O. A. (2007) *J. Biol. Chem.* **282,** 14515–14524
45. Altiok, S., Xu, M., and Spiegelman, B. M. (1997) *Genes Dev.* **11,** 1987–1998
46. Wang, H., Iakova, P., Wilde, M., Welm, A., Goode, T., Roesler, W. J., and Timchenko, N. A. (2001) *Mol. Cell* **8,** 817–828
47. Chen, P. L., Riley, D. J., Chen, Y., and Lee, W. H. (1996) *Genes Dev.* **10,** 2794–2804
48. Cole, K. A., Harmon, A. W., Harp, J. B., and Patel, Y. M. (2004) *Am. J. Physiol. Cell Physiol.* **286,** C349–C354
49. Sebastian, T., Malik, R., Thomas, S., Sage, J., and Johnson, P. F. (2005) *EMBO J.* **24,** 3301–3312
50. Gulbagci, N. T., Li, L., Ling, B., Gopinadhan, S., Walsh, M., Rossner, M., Nave, K. A., and Taneja, R. (2009) *EMBO Rep.* **10,** 79–86
51. Kanichai, M., Ferguson, D., Prendergast, P. J., and Campbell, V. A. (2008) *J. Cell. Physiol.* **216,** 708–715
52. Amarilio, R., Viukov, S. V., Sharir, A., Eshkar-Oren, I., Johnson, R. S., and Zelzer, E. (2007) *Development* **134,** 3917–3928
53. Simon, M. C., and Keith, B. (2008) *Nat. Rev. Mol. Cell Biol.* **9,** 285–296